Agonist-induced formation of unproductive receptor-G$_{12}$ complexes

Najeah Okashah[a] , Shane C. Wright[b] , Kouki Kawakami[c], Signe Mathiasen[d,e,f], Joris Zhou[b], Sumin Lu[a], Jonathan A. Javitch[d,e,f] , Asuka Inoue[c], Michel Bouvier[b] , and Nevin A. Lambert[a,1]

[a]Department of Pharmacology and Toxicology, Medical College of Georgia, Augusta University, Augusta, GA 30912; [b]Institute for Research in Immunology and Cancer, Department of Biochemistry and Molecular Medicine, Université de Montréal, Montréal, QC H3T 1J4, Canada; [c]Graduate School of Pharmaceutical Sciences, Tohoku University, 980-8578 Sendai, Japan; [d]Department of Psychiatry, Columbia University Vagelos College of Physicians and Surgeons, New York, NY 10032; [e]Department of Pharmacology, Columbia University Vagelos College of Physicians and Surgeons, New York, NY 10032; and [f]Division of Molecular Therapeutics, New York State Psychiatric Institute, New York, NY 10032

G proteins are activated when they associate with G protein-coupled receptors (GPCRs), often in response to agonist-mediated receptor activation. It is generally thought that agonist-induced receptor-G protein association necessarily promotes G protein activation and, conversely, that activated GPCRs do not interact with G proteins that they do not activate. Here we show that GPCRs can form agonist-dependent complexes with G proteins that they do not activate. Using cell-based bioluminescence resonance energy transfer (BRET) and luminescence assays we find that vasopressin V$_2$ receptors (V$_2$R) associate with both G$_s$ and G$_{12}$ heterotrimers when stimulated with the agonist arginine vasopressin (AVP). However, unlike V$_2$R-G$_s$ complexes, V$_2$R-G$_{12}$ complexes are not destabilized by guanine nucleotides and do not promote G$_{12}$ activation. Activating V$_2$R does not lead to signaling responses downstream of G$_{12}$ activation, but instead inhibits basal G$_{12}$-mediated signaling, presumably by sequestering G$_{12}$ heterotrimers. Overexpressing G$_{12}$ inhibits G protein receptor kinase (GRK) and arrestin recruitment to V$_2$R and receptor internalization. Formyl peptide (FPR1 and FPR2) and Smoothened (Smo) receptors also form complexes with G$_{12}$ that are insensitive to nucleotides, suggesting that unproductive GPCR-G$_{12}$ complexes are not unique to V$_2$R. These results indicate that agonist-dependent receptor-G protein association does not always lead to G protein activation and may in fact inhibit G protein activation.

GPCR | ternary complex | G protein-coupled receptor | arrestin

G protein-coupled receptors (GPCRs) mediate important physiological activities and exert most of their effects through activation of G proteins. In the conventional model of coupling, unliganded receptors are poor recruiters and activators of G proteins, whereas agonist-bound GPCRs take on more active conformations that effectively recruit G protein heterotrimers (1, 2). Productive receptor-G protein association promotes GDP release by stabilizing the nucleotide-free state of the Gα subunit, which in turn allows GTP binding, G protein activation, and downstream signaling (3, 4). According to this model, agonist-dependent GPCR-G protein complex formation is essentially synonymous with G protein activation. Four families of G proteins (G$_s$, G$_{i/o}$, G$_{q/11}$, and G$_{12/13}$) can be activated, and each leads to a distinct set of downstream signaling outcomes. It is generally thought that selection of G protein subtypes by GPCRs occurs at the receptor-G protein association step, such that receptors interact with and activate cognate G protein subtypes and do not interact with noncognate G protein subtypes. Here we find that agonist-dependent GPCR-G protein association can occur without promoting subsequent G protein activation, thus, whether a G protein subtype is activated can be determined after initial receptor-G protein engagement. Moreover, noncognate G proteins can impede downstream events, perhaps by competing with other intracellular transducers for access to activated receptors. These findings revise the standard model of G protein coupling by indicating that agonist-induced GPCR-G protein association does not always promote G protein activation and may in some circumstances inhibit downstream signaling.

Results

V$_2$R Interacts with G$_{12}$ Heterotrimers. Conventional GPCR-G protein coupling is understood as an allosteric interaction where an agonist-bound active receptor mediates GDP release by stabilizing the nucleotide-free state of an associated Gα subunit (3–5). Receptor complexes with nucleotide-free G proteins are quite transient when guanine nucleotides are present at concentrations similar to those found in cells, but are stabilized when guanine nucleotides are absent. In order to observe allosteric coupling we monitored receptor-G protein association under conditions that allowed us to control both ligand binding to the receptor and nucleotide binding to the G protein. We used bioluminescence resonance energy transfer (BRET) between GPCRs fused to *Renilla* luciferase (Rluc8) and Gβ$_1$ and Gγ$_2$ subunits fused to complementary fragments of Venus fluorescent protein (6–8) to monitor receptor-G protein association. These components and unlabeled Gα subunits were transfected into HEK 293 cells in which most of the endogenous G proteins had been deleted using CRISPR/Cas9-mediated gene editing (9, 10). In order to control nucleotide binding to G proteins, cells were permeabilized and either supplemented with nucleotides or treated with apyrase to remove residual nucleotides.

Significance

G protein-coupled receptors (GPCRs) are targeted by a large fraction of approved drugs and regulate many important cellular processes. Association of GPCRs with heterotrimeric G proteins in response to agonist activation is thought to invariably lead to G protein activation. We find instead that G$_{12}$ heterotrimers can associate with agonist-bound receptors in a manner that does not lead to activation. These unproductive agonist–receptor-G protein ternary complexes sequester G$_{12}$ heterotrimers and thus inhibit rather than support G$_{12}$ signaling. These findings reveal a mechanism whereby agonist activation of GPCRs can inhibit as well as promote G protein signaling.

PHARMACOLOGY

Because receptor-G protein complexes are transient it can be difficult to detect agonist-induced BRET signals between receptors and G proteins when guanine nucleotides are present (6). For example, arginine vasopressin (AVP) did not detectably increase BRET between vasopressin V_2 receptors (V_2R) and G_s heterotrimers in the presence of GDP (Fig. 1A). In contrast, AVP produced large BRET increases in the absence of nucleotides (Fig. 1A). Stabilization of agonist–receptor-G protein complexes when $G\alpha$ subunits are nucleotide-free indicates conventional "productive" allosteric coupling and predicts that agonist-bound receptors will promote GDP release and G protein activation under physiological conditions. Nucleotide-free conditions also enhanced AVP-induced BRET between V_2R and G_{i1} or G_q heterotrimers (*SI Appendix*, Fig. S1). These results are consistent with cognate V_2R activation of G_s and G_q heterotrimers (11, 12) and predict some ability to activate G_{i1} heterotrimers. In contrast, we

observed surprisingly robust agonist-induced BRET between V_2R and G_{12} heterotrimers in the presence of GDP that was not enhanced by nucleotide depletion (Fig. 1A). These results suggest that AVP-bound V_2R can form complexes with GDP-bound G_{12} heterotrimers that do not progress to the nucleotide-free state and therefore are not stabilized when GDP is removed (Fig. 1B). As an index of allosteric coupling we divide the increase in BRET produced by agonist in the presence of GDP ($\Delta BRET_{ag}$) by the increase in BRET produced by the combined effect of agonist and nucleotide depletion ($\Delta BRET_{ag+apy}$), and refer to this index as the GDP-resistance ratio, or R_{GDP}. R_{GDP} values that are less than 1 indicate conventional productive coupling, whereas an R_{GDP} value of 1 indicates nucleotide-resistant or unproductive coupling. R_{GDP} for V_2R and G_s was 0.08 ± 0.12 (mean $\pm$ SD; $n = 6$), whereas R_{GDP} for V_2R and G_{12} was 1.01 ± 0.06 ($n = 6$). In contrast to V_2R, we observed more conventional productive coupling of both endothelin A (ET_A) and thromboxane A_2 (TP) receptors with G_{12} heterotrimers, with R_{GDP} values of 0.66 ± 0.09 ($n = 3$) and 0.55 ± 0.09 ($n = 6$), respectively. Both of these receptors also coupled productively with G_q heterotrimers, with R_{GDP} values of 0.29 ± 0.08 ($n = 3$) and 0.11 ± 0.07 ($n = 6$), respectively (*SI Appendix*, Fig. S2).

Receptors that couple to one member of a $G\alpha$ subunit family can usually couple to other members of the same family. Therefore, we examined V_2R coupling to G_{13} heterotrimers, the other member of the $G_{12/13}$ family (13). We found that stimulation with AVP increased BRET between V_2R and G_{13} heterotrimers in the presence of GDP (*SI Appendix*, Fig. S3). However, unlike what we observed with G_{12}, these responses were enhanced by nucleotide depletion ($R_{GDP} = 0.67 \pm 0.08$; $n = 4$), indicating productive coupling, consistent with weak V_2R-mediated activation of G_{13} (14). Similar results were obtained with G_{13} heterotrimers and ET_A ($R_{GDP} = 0.21 \pm 0.03$; $n = 4$) and TP ($R_{GDP} = 0.18 \pm 0.01$; $n = 4$) receptors (*SI Appendix*, Fig. S3).

Because nucleotide-resistant V_2R-G_{12} association was unexpected we performed additional experiments to rule out the possibility that our standard BRET assay was simply detecting an agonist-induced change in V_2R-Rluc8 conformation. We reasoned that if both ET_A and V_2R receptors were able to associate with G_{12} the two receptors should compete for a common pool of heterotrimers. Indeed, we found that stimulation of unlabeled ET_A receptors inhibited AVP-induced BRET between V_2R-Rluc8 and G_{12} heterotrimers in intact cells (*SI Appendix*, Fig. S4A). Conversely, stimulation of unlabeled V_2R receptors inhibited endothelin-1–induced BRET between ET_A-Rluc8 and G_{12} heterotrimers (*SI Appendix*, Fig. S4B). Second, we found that stimulation of unlabeled V_2R receptors increased BRET between $G\alpha_{12}$-Rluc8 and $G\beta\gamma$-Venus in intact cells (*SI Appendix*, Fig. S5 A and B). This increase persisted in permeabilized cells that were treated with apyrase and supplemented with GDPβS to prevent the possibility of heterotrimer activation by residual GTP (*SI Appendix*, Fig. S5B). This suggests that active V_2R receptors may impose a conformational change in G_{12} heterotrimers that does not require GTP binding or G_{12} activation. In contrast, stimulation of unlabeled ET_A and TP receptors decreased BRET between $G\alpha_{12}$-Rluc8 and $G\beta\gamma$-Venus, and these decreases were largely blocked in permeabilized cells when only GDPβS was present (*SI Appendix*, Fig. S5C). Finally, we found that AVP increased luciferase complementation when a small fragment (SmBit) of Nanoluc was fused to V_2R, and a large fragment of Nanoluc was fused to $G\gamma_2$, and these proteins were coexpressed with unlabeled $G\alpha_{12}$ and $G\beta_1$ (*SI Appendix*, Fig. S6). These results are consistent with AVP-induced association of V_2R receptors and G_{12} heterotrimers.

Additional experiments revealed that V_2R recruited G_s and G_{12} heterotrimers at similar rates (Fig. 1C) and that agonist-induced V_2R-G_{12} complexes were equally stable in the presence of GDP or GTP (Fig. 1D). Stimulation of V_2R with the agonist oxytocin produced similar responses to AVP, indicating
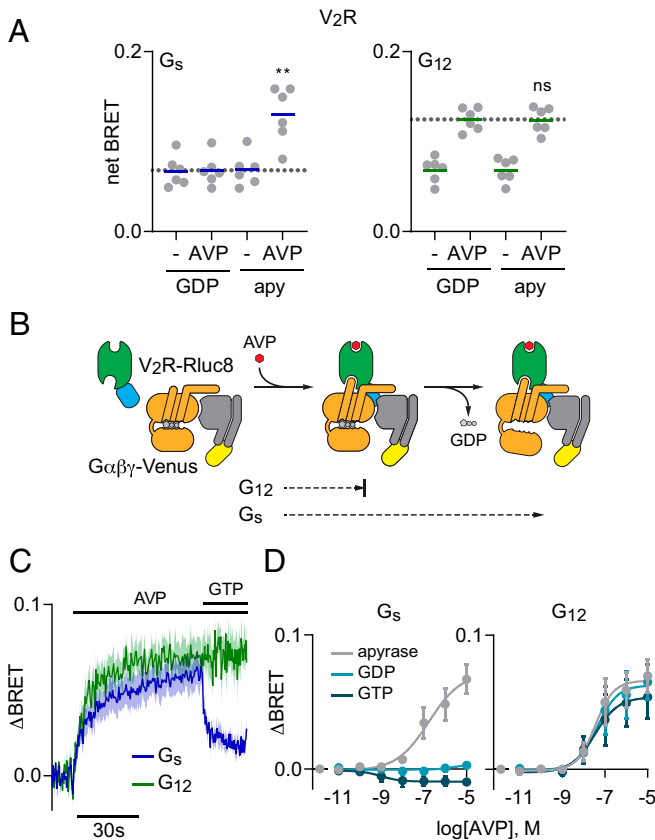

Fig. 1. V_2R forms GDP-resistant agonist-induced complexes with G_{12} heterotrimers. (*A*) BRET between V_2R-Rluc8 and $G\alpha\beta\gamma$-Venus in the presence or absence of AVP (1 μM), and the presence or absence of GDP. When GDP was absent, apyrase (apy) was added to remove residual nucleotides. AVP-induced BRET to G_s (*Left*) but not G_{12} (*Right*) heterotrimers was enhanced when GDP was absent; **$P < 0.005$; n.s., not significant ($P = 0.58$); one-way ANOVA (Sidak's test) compared to GDP+AVP; $n = 6$. (*B*) Cartoon representation of two steps of V_2R-G protein coupling: agonist-induced formation of receptor-G protein complexes, and GDP release. (*C*) Time course of BRET between V_2R-Rluc8 and $G\alpha\beta\gamma$-Venus in response to injection of 1 μM AVP, followed by injection of 100 μM GTP in permeabilized cells treated with apyrase (mean $\pm$ SEM; $n = 4$–6). (*D*) BRET between V_2R-Rluc8 and $G\alpha\beta\gamma$-Venus as a function of AVP concentration in permeabilized cells expressing either G_s (*Left*) or G_{12} (*Right*) heterotrimers treated with apyrase, GDP (100 μM), or GTP (100 μM). The logEC$_{50}$ for association with G_s is -6.8 ± 0.5 in apyrase-treated cells, and the logEC$_{50}$s for association with G_{12} were -7.5 ± 0.3, -7.4 ± 0.4, and -7.5 ± 0.5 in the presence of apyrase, GDP, and GTP, respectively. Data points represent the change in BRET ($\Delta BRET$) in response to AVP (mean $\pm$ SEM; $n = 3$).

that nucleotide-insensitive V$_2$R-G$_{12}$ interactions are not restricted to AVP (*SI Appendix*, Fig. S7*A*), and AVP-induced responses were inhibited by the antagonist mozavaptan (*SI Appendix*, Fig. S7*B*).

V$_2$R Does Not Activate G$_{12}$ Heterotrimers. The above results suggested that AVP-stimulated V$_2$R should not activate G$_{12}$ heterotrimers. To test this prediction we turned to sensitive assays that monitor signaling downstream of G$_{12}$ activation. We first monitored translocation of full-length p115-RhoGEF and a fragment (amino acids 281–483) of PDZ-RhoGEF from the cytosol to the plasma membrane using bystander BRET assays (15, 16). These proteins bind to activated Gα_{12} subunits at the plasma membrane to regulate Rho GTPase activity and actin fiber formation (17, 18). ET$_A$ and TP receptors robustly recruited p115-RhoGEF to the plasma membrane in a G$_{12}$-dependent manner (Fig. 2*A*). In contrast, stimulation of V$_2$R receptors failed to recruit p115-RhoGEF and instead decreased the baseline abundance of this reporter at the plasma membrane (Fig. 2*A*). Similar results were obtained with V$_2$R and TP receptors and

PDZ-RhoGEF recruitment to the plasma membrane (Fig. 2*B*) and direct recruitment of the RGS homology domain (amino acids 1–246) of p115-RhoGEF, p115-RGS-GFP, to Gα_{12}-RlucII (Fig. 2*C*). The AVP-induced decrease in p115-and PDZ-RhoGEF at the plasma membrane suggests that active V$_2$R may sequester G$_{12}$ heterotrimers, preventing activation by endogenous receptors. Consistent with this suggestion, we found that activation of V$_2$R could significantly reduce p115-RhoGEF recruitment mediated by activation of ET$_A$ receptors (Fig. 2*D*). A second sensitive assay of G$_{12}$ activity is gene transcription driven by activation of the serum response element (SRE) (19). Stimulation of V$_2$R receptors failed to activate SRE-dependent gene transcription, whereas stimulation of both ET$_A$ and TP receptors could activate SRE in a G$_{12}$-dependent manner (Fig. 2*E*). A similar trend was observed with transcription driven by nuclear factor kappa-light-chain enhancer of activated B cells (NFκB; Fig. 2*F*). These results demonstrate that active V$_2$R receptors do not detectably activate G$_{12}$ heterotrimers, even though the two proteins interact in an agonist-dependent manner.
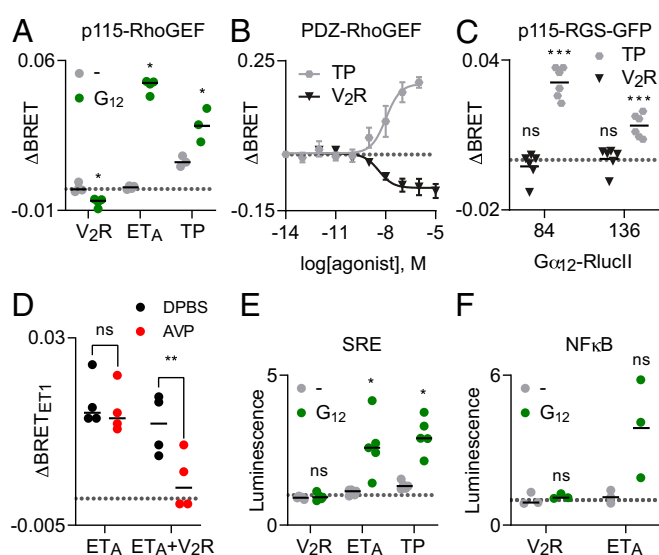
V$_2$R Activates G$_{12}$ Chimeras and Mutants. Canonical GPCR-mediated activation of G proteins involves extension of the Gα subunit C terminus (helix 5; H5) into the active receptor core (20, 21). This region of Gα is necessary for productive coupling and is also a key determinant of receptor-G protein selectivity. Therefore, we hypothesized that exchanging the Gα_{12} C terminus with C-terminal peptides from other Gα subunits might allow productive coupling with V$_2$R. Indeed, we found that Gα_{12} chimeras bearing the last 10 amino acids of either Gα_s or Gα_q (Fig. 3*A*) interacted with AVP-activated V$_2$R in a GDP-sensitive manner; R$_{GDP}$ values were significantly less than 1 for G$_{12s}$ and G$_{12q}$ heterotrimers and were similar to R$_{GDP}$ for G$_s$ and G$_q$ heterotrimers (Fig. 3*B*). G$_{12s}$ and G$_{12q}$ chimeras also supported V$_2$R-mediated translocation of p115-RhoGEF to the plasma membrane, consistent with productive coupling to these heterotrimers and activation of G$_{12}$ signaling pathways (Fig. 3*C*). Conversely, we found that replacing the C-terminal peptides of either Gα_s or Gα_q with that of Gα_{12} (Fig. 3*A*) dramatically increased R$_{GDP}$, indicating much less productive coupling to G$_{s12}$ and unproductive coupling to G$_{q12}$ (Fig. 3*B*). We next made point mutations in the Gα_{12} C terminus to introduce residues with properties shared by the corresponding residues in Gα_s and Gα_q (Fig. 3*A*). We found that Gα_{12} mutants with a hydrophobic residue in the −1 position (Q381L and Q381V) still coupled unproductively with V$_2$R (Fig. 3 *D* and *E*). In contrast, Gα_{12} mutants with a tyrosine in the −4 position (I378Y) coupled productively with V$_2$R; R$_{GDP}$ was less than 1 (Fig. 3*D*), and I378Y supported V$_2$R-mediated translocation of p115-RhoGEF (Fig. 3*E*). Similar weak but productive coupling to V$_2$R was observed when Gα_{12} was simply truncated by a single amino acid (Δ1; Fig. 3 *D* and *E*). These results indicate that the Gα_{12} C terminus is required for unproductive coupling to active V$_2$R. Together with the observation that subtle modifications of the Gα_{12} C terminus overcome the barrier to productive coupling, this result suggests that G$_{12}$ heterotrimers are likely to interact with active V$_2$R in a manner that is structurally similar to canonical GPCR-G protein complexes.

The V$_2$R-G$_{12}$ Interaction Interferes with Other Transducers. The robust agonist-induced BRET signal between V$_2$R receptors and G$_{12}$ heterotrimers in the presence of nucleotides suggested that this interaction might be stable enough to interfere with recruitment of other intracellular transducer molecules to V$_2$R. As V$_2$R receptors canonically activate G$_s$ heterotrimers (11), we first asked how overexpressing G$_{12}$ would influence activation of adenylyl cyclase and cAMP accumulation. We found that overexpressing G$_{12}$ resulted in modest inhibition of G$_s$ activation, as
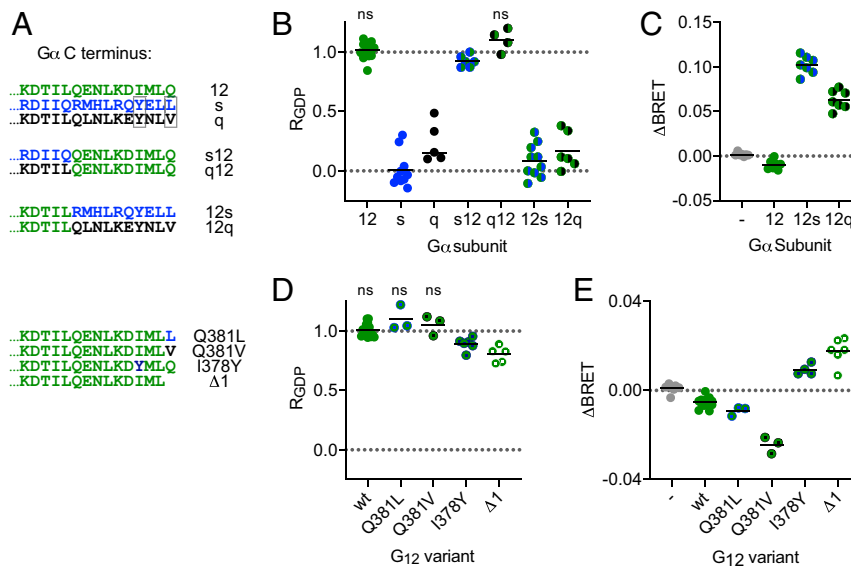

Fig. 2. V$_2$R does not activate G$_{12}$ heterotrimers. (*A*) Activation of V$_2$R decreases bystander BRET between p115RhoGEF-Rluc8 and the plasma membrane marker Venus-Kras when G$_{12}$ is expressed, whereas activation of ET$_A$ and TP receptors increases this signal, indicating association of p115RhoGEF-Rluc8 and active Gα_{12} at the plasma membrane; *P < 0.05; paired *t* test compared to mock-transfected control (–); *n* = 3–4. (*B*) V$_2$R activation decreases BRET between PDZ-RhoGEF-RlucII and the plasma membrane marker rGFP-CAAX, whereas TP activation increases this signal (mean ± SEM; *n* = 3). (*C*) TP activation increases BRET between two different Gα_{12}-RlucII constructs and p115-RGS-GFP, whereas V$_2$R activation has no effect on this signal; ***P < 0.0005; n.s., not significant; one-sample *t* test compared to zero; *n* = 6. RlucII was fused to Gα_{12} after amino acids 84 and 136 in the two different probes. Data points in *A*–*C* represent the change in BRET (ΔBRET) in response to agonist, and the broken gray line represents zero. (*D*) Activation of V$_2$R reduces p115-RhoGEF recruitment mediated by activation of ET$_A$. Activation of ET$_A$ (ET1; 100 nM) increases BRET between p115RhoGEF-Rluc8 and Venus-Kras, and this response is significantly inhibited when V$_2$R receptors are coexpressed and activated (AVP; 1 μM); n.s., not significant (P = 0.43); **P < 0.005; one-way ANOVA (Sidak's test); *n* = 4. Data points represent the change in bystander BRET (ΔBRET) in response to ET1, and the broken gray line represents zero. (*E*) Activation of V$_2$R fails to activate the SRE when G$_{12}$ is expressed, whereas activation of ET$_A$ and TP receptors increases SRE-driven gene expression; *P < 0.05; n.s., not significant; paired *t* test compared to (–); *n* = 5. (*F*) V$_2$R receptors fail to activate NFκB-driven gene expression when G$_{12}$ is expressed; n.s., not significant; paired *t* test compared to (–); *n* = 3. Data points in *E* and *F* represent luminescence normalized to vehicle-treated controls, and the broken gray line represents one (no change). Agonists were AVP (1 μM), ET1 (100 nM), and U-46619 (10 μM).

Fig. 3. Role of the $G\alpha_{12}$ C terminus in unproductive coupling with V_2R. (A) Amino acid sequences of the distal C terminus of $G\alpha_{12}$ (*green*), $G\alpha_s$ (*blue*), $G\alpha_q$ (*black*), and the chimeras and mutants used in *B–E*. Boxes indicate residues whose properties are shared between $G\alpha_s$ and $G\alpha_q$ but not $G\alpha_{12}$. (B) GDP resistance (R_{GDP}) of interactions between V_2R-Rluc8 and heterotrimers incorporating the indicated $G\alpha$ subunits; n.s., not significant; all other groups significantly different from one; $P < 0.05$; one-sample t test; $n = 4$–10. (C) Activation of V_2R decreases bystander BRET between p115RhoGEF-Rluc8 and Venus-Kras when G_{12} is expressed, but increases bystander BRET when G_{12s} or G_{12q} are expressed, indicating receptor-mediated activation of these chimeras; all groups were significantly different from mock-transfected controls (–); $P < 0.05$; one-way ANOVA (Dunnett's test); $n = 7$. (D) GDP resistance of interactions between V_2R-Rluc8 and G_{12} heterotrimers bearing the indicated point mutations; n.s., not significant; all other groups significantly different from one; $P < 0.05$; one-sample t test; $n = 3$–14. (E) Activation of V_2R decreases p115RhoGEF-Rluc8 translocation when G_{12} wt, Q381L, or Q381V are expressed, but increases translocation when G_{12} I378Y or $\Delta 1$ are expressed; all groups were significantly different from mock-transfected controls (–); $P < 0.05$; one-way ANOVA (Dunnett's test); $n = 3$–13.

indicated by a G_s biosensor (*SI Appendix*, Fig. S8A). Surprisingly, this did not lead to detectable inhibition of V_2R-mediated cAMP accumulation, as indicated by two different cAMP sensors (*SI Appendix*, Fig. S8 *B* and *C*). Active V_2R receptors are phosphorylated by G protein receptor kinases (GRKs), and phosphorylated V_2R bind tightly to β-arrestins (22). Remarkably, we found that overexpressing G_{12} significantly reduced AVP-induced BRET between V_2R-Rluc8 and β-arrestin2–Venus (Fig. 4 *A* and *B*). A much smaller but still significant reduction was observed after overexpressing G_s heterotrimers (Fig. 4 *A* and *B*). In contrast, overexpressing G_{12} did not significantly reduce β-arrestin2 recruitment to ET_A, β$_2$-adrenergic, or angiotensin AT_1 receptors (*SI Appendix*, Fig. S9). Because V_2R–β-arrestin interactions are very stable and because phosphorylated V_2R can accommodate G protein and arrestin binding simultaneously (23), we suspected that G_{12} overexpression was acting upstream of arrestin binding to inhibit V_2R interactions with GRKs. Consistent with this hypothesis, we found that G_{12} overexpression greatly reduced the AVP-induced interaction of V_2R and GRK2 (*SI Appendix*, Fig. S10). Because arrestin binding is critical for agonist-dependent V_2R internalization (22) we then asked if G_{12} overexpression would inhibit receptor endocytosis. Indeed, overexpression of G_{12} but not G_s heterotrimers inhibited V_2R trafficking from the plasma membrane to the endosomal compartment as assessed by enhanced bystander BRET (ebBRET; Fig. 4 *C* and *D*). Conversely, there was a small but significant enhancement of V_2R internalization in cells lacking $G\alpha_{12}$ and $G\alpha_{13}$ subunits (*SI Appendix*, Fig. S11).

Other Receptors Also Form Unproductive Complexes with G_{12}. In the course of experiments examining coupling of multiple different GPCRs to G proteins we encountered three additional examples of receptors that interact with G_{12} heterotrimers in a nucleotide-resistant, unproductive manner. Smoothened (Smo) displays constitutive activity when the sterol transporter Patched is inhibited

by Hedgehog or is not present, as is the case in HEK 293 cells. Smo is known to couple to and activate G_i heterotrimers (24). We found that unliganded Smo-Rluc8 did indeed interact with G_i heterotrimers in BRET assays, and this interaction was inhibited by either the inverse agonist cyclopamine or GDP, indicative of productive coupling ($R_{GDP} = 0.19 \pm 0.10$; $n = 3$). In contrast, BRET between Smo-Rluc8 and G_{12} heterotrimers was inhibited by cyclopamine but not GDP, indicative of unproductive coupling ($R_{GDP} = 1.01 \pm 0.22$; $n = 3$; Fig. 5A). Similarly, activation of formyl peptide 2 receptors (FPR2) with the agonist peptide WKYMVm (WKY) promoted productive coupling with G_i heterotrimers ($R_{GDP} = 0.30 \pm 0.07$; $n = 4$), but unproductive coupling with G_{12} heterotrimers ($R_{GDP} = 0.92 \pm 0.04$; $n = 4$; Fig. 5B). Although neither of these two receptors is known to activate G_{12} we directly assessed activation of downstream G_{12} signaling pathways by FPR2. As was the case with V_2R, activation of FPR2 failed to recruit p115-RhoGEF to the plasma membrane and failed to activate SRE-dependent gene transcription (*SI Appendix*, Fig. S12). Formyl peptide 1 receptors (FPR1) are highly homologous with FPR2 (68% identical), and we found that FPR1 also coupled productively with G_i heterotrimers ($R_{GDP} = 0.26 \pm 0.01$; $n = 3$), but unproductively with G_{12} heterotrimers ($R_{GDP} = 0.96 \pm 0.02$; $n = 3$).

When we examined association of GPCRs with G proteins from all four $G\alpha$ subtype families, we found that highly GDP-resistant interactions ($R_{GDP} > 0.5$) were restricted to G_{12} heterotrimers (Fig. 6). For 19 of the 20 interactions that were studied with G_s, G_i, and G_q heterotrimers, R_{GDP} was <0.3, whereas this was the case for only two of the nine interactions we studied with G_{12} heterotrimers. These results suggest that receptor-G_{12} complexes may generally be more stable than other receptor-G protein complexes when G proteins are bound to GDP.
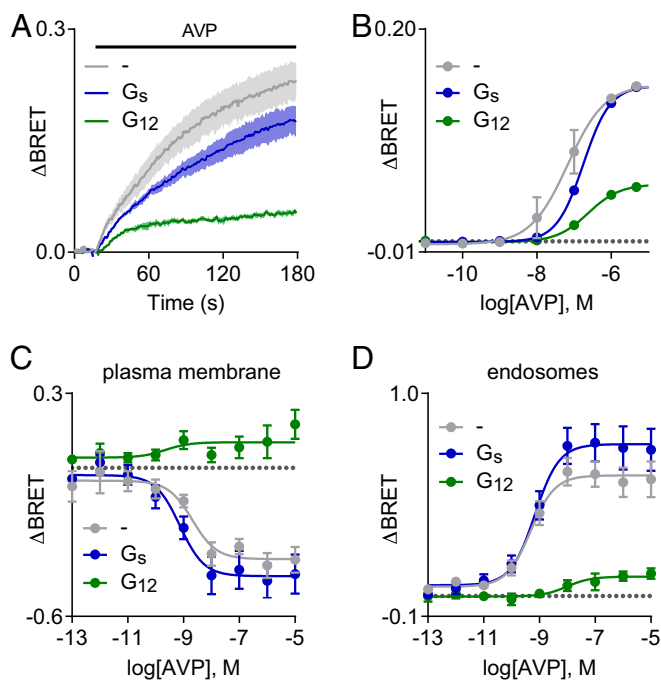
Fig. 4. Overexpression of G_{12} inhibits arrestin recruitment to V_2R and receptor internalization. (*A* and *B*) Time course and concentration-dependence of BRET between V_2R-Rluc8 and β-arrestin2–Venus in response to AVP (1 μM in *A*; mean ± SEM; *n* = 3). Overexpression of G_{12} but not G_s heterotrimers inhibits arrestin recruitment. (*C* and *D*) AVP-induced changes in BRET between V_2R-RlucII and the plasma membrane marker rGFP-CAAX (*C*) and the endosome marker rGFP-FYVE (*D*), indicating trafficking of V_2R-RlucII from the plasma membrane to endosomes (mean ± SEM; *n* = 6–8). Overexpression of G_{12} but not G_s heterotrimers inhibits AVP-induced internalization of V_2R-RlucII.

Discussion

Taken together, our results suggest that several GPCRs bind to G_{12} heterotrimers in an activation-dependent manner, but the resulting GPCR-G_{12} complexes are insensitive to guanine nucleotides. These interactions do not activate G_{12} signaling, but may instead have a negative effect on RhoGEF recruitment and signaling by sequestering G_{12}, thus preventing activation by other receptors. These interactions may also interfere with recruitment of other intracellular transducers and thus change signaling or trafficking of receptors that recruit but fail to activate G_{12} heterotrimers. Whether or not these inhibitory effects occur under physiological conditions will depend on several factors, most notably the local abundance of G_{12} heterotrimers and the stoichiometry of receptors and intracellular transducers. The normal physiological role of the V_2R is to enhance water reabsorption in the kidney by stimulating G_s, which ultimately leads to incorporation of aquaporin-2 water channels to the luminal surface of collecting duct cells (25). An inhibitory effect of V_2R activation on G_{12} signaling could conceivably contribute to the physiological activity of this receptor, as Rho activity has been reported to act as an inhibitor of aquaporin transport (26). An inhibitory effect of the V_2R-G_{12} interaction on arrestin recruitment could also play a regulatory role to limit receptor internalization. Although we found that G_{12} overexpression weakly inhibited V_2R-mediated G_s activation when assessed using a direct G_s activation assay, we were surprised to find that this did not lead to a detectable decrease in cAMP accumulation. It is possible that GRK and arrestin recruitment are more sensitive to competition with G_{12} than cAMP accumulation because cAMP signals are amplified downstream of G_s. Similar observations have

been made after expression of some intrabodies that recognize the active state of β2-adrenergic receptors (27). Further studies with native systems will be required to determine if unproductive GPCR-G_{12} association has physiological significance.

At present, our findings significantly change the current model of GPCR coupling by demonstrating robust agonist-induced receptor-G protein interactions that do not lead to nucleotide exchange and G protein activation. GPCRs are thought to have access to all G protein subtypes expressed in a given cell, but possible interactions with noncognate heterotrimers (defined as G proteins that cannot be activated by a given GPCR) have, with a few exceptions (28), been overlooked. It is commonly assumed that stable agonist-induced GPCR-G protein interactions are restricted to cognate G proteins and are associated with G protein activation. One implication of this idea is that the conventional selection process whereby receptors reject noncognate G proteins occurs at an early stage of receptor-G protein association, such that complexes with noncognate G proteins do not progress past weak and transient encounter complexes. This seems to be true in the majority of cases, as several previous studies using sensitive methods have shown that interactions between GPCRs and noncognate G proteins are usually undetectable (7, 29). In contrast, our results suggest that some receptors functionally reject G_{12} heterotrimers despite forming relatively stable GPCR-G_{12} complexes. It is thought that GPCR-G protein complexes evolve through multiple intermediate conformations prior to receptor-stimulated nucleotide release (30–34). It is possible that receptors such as V_2R and FPR2 form similar intermediate complexes with G_{12} heterotrimers that are unusually stable (Fig. 1*B*) and are unable to promote the changes in G_{12} that lead to GDP release. Spontaneous GDP release from
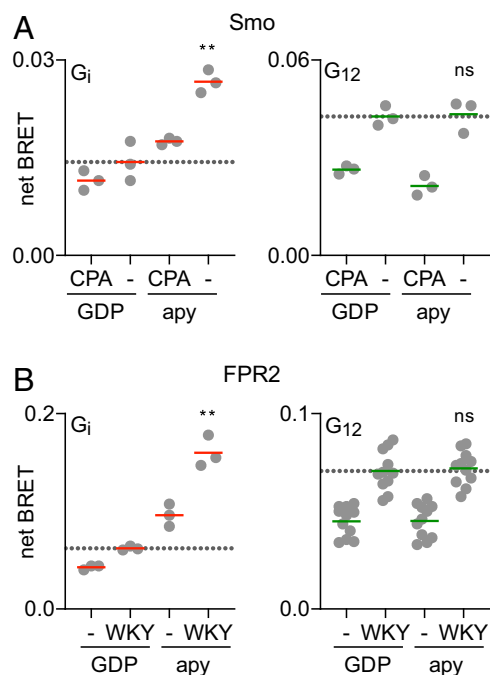

Fig. 5. Smo and FPR2 form GDP-resistant complexes with G_{12} heterotrimers. (*A*) BRET between Gαβγ-Venus heterotrimers and Smo-Rluc8 in the presence and absence of the inverse agonist cyclopamine (CPA; 10 μM), in the presence and absence of GDP. Smo is constitutively active in the absence of CPA. (*B*) BRET between Gαβγ-Venus heterotrimers and FPR2-Rluc8 in the presence and absence of the agonist WKYMVm (WKY, 0.5 μM), in the presence and absence of GDP. Both receptors coupled productively to G_{i1} heterotrimers, but unproductively to G_{12} heterotrimers; **$P < 0.005$; n.s., not significant ($P > 0.75$); one-way ANOVA (Sidak's test) compared to GDP-CPA (*A*) and GDP+WKY (*B*); *n* = 3–12.
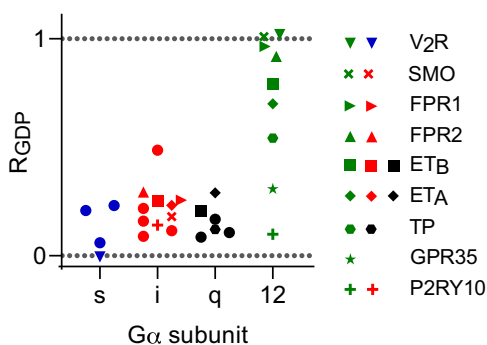
Fig. 6. Receptor interactions with G_{12} heterotrimers demonstrate a wide range of sensitivity to GDP. GDP resistance (R_{GDP}) of interactions between a panel of GPCRs fused to Rluc8 and the indicated $G\alpha\beta\gamma$-Venus heterotrimers (mean; $n = 3–6$). Receptors that interact in an agonist-dependent manner with G_{12} heterotrimers are individually identified. Additional receptors are indicated by closed circles, and include: β_2AR, H_2R, D_1R (with G_s), α_2AR, M_4R, A_1R, D_2R, MOR (with G_i), AT_1R, M_3R, H_1R (with G_q). A full listing of receptor genes and ligands is provided in *SI Appendix*, Table S1.

G_{12} heterotrimers is particularly slow (35), and it may be that receptor-mediated GDP release requires relatively stable complexes with G_{12}-GDP, even for receptors that do activate G_{12}. G protein chimeras and mutants revealed that the $G\alpha_{12}$ C terminus is necessary for unproductive complexes with V_2R, implying that these complexes share some structural features with conventional productive ternary complexes. Our results with intramolecular G_{12} BRET sensors suggest that V_2R and FPR2 may promote conformational changes in G_{12} that do not lead to activation. However, the resolution of such probes is insufficient to determine if the heterotrimer itself changes conformation or, alternatively, if only the attached BRET donor and acceptor labels are rearranged. In either case, these results suggest that changes in G protein conformation reported by sensors similar to those used here do not necessarily indicate G protein activation.

In summary, our results reveal a mode of GPCR-G protein interaction wherein agonist-activated receptors bind to G_{12} heterotrimers but do not promote nucleotide exchange and activation. These findings show that receptors can inhibit as well as activate G proteins, adding to the complexity of GPCR-mediated signaling.

Materials and Methods

Materials. Trypsin, DPBS, PBS, HBSS, FBS, MEM, DMEM, penicillin/streptomycin, and L-glutamine were from Gibco (ThermoFisher Scientific). Polyethyleneimine MAX (PEI MAX) was purchased from Polysciences, Inc. Some receptor ligands, luciferin-D, and forskolin were purchased from Cayman Chemical. The remaining receptor ligands, digitonin, apyrase, GDP, GTP, GDPβS, and GTPγS were purchased from MilliporeSigma. Coelenterazine h and coelenterazine 400a were purchased from Nanolight Technologies. NanoGlo luciferase substrate was purchased from Promega.

Plasmid DNA Constructs. GPCR plasmids were purchased from cdna.org (Bloomsburg University) or were provided by Bryan Roth (PRESTO-Tango Kit - #1000000068, Addgene). The V_2R-Rluc8 plasmid was received as a gift from Kevin Pfleger (Harry Perkins Institute of Medical Research, Nedlands, Western Australia). A plasmid encoding β-arrestin2–Venus was a gift from Vsevolod Gurevich (Vanderbilt University, Nashville, TN). V_2R-SmBit and ETAR-SmBit were generated by replacing the GPCR coding sequence in β_2AR-SmBit digested with *EcoRI* and *NotI*, which appended the SmBit peptide to the C terminus of each receptor behind a GGRGGGGSG linker. Plasmids encoding $G\alpha$ subunits, $G\beta_1$, and $G\gamma_2$ were purchased from cdna.org. $G\alpha_{12}$-Rluc8 was generated by inserting Rluc8 (flanked by GGSG linkers) between a residues N136 and K137 of $G\alpha_{12}$ using Quikchange mutagenesis. GRK2-Venus-Kras and GRK2-Venus-Kras R587Q were generated by appending Venus fused to the last 25 amino acids of Kras to the C terminus of bovine GRK2 or GRK2 R587Q using Quikchange mutagenesis. Plasmids encoding the S1 subunit of

pertussis toxin (PTX-S1) and LgBit-$G\gamma_2$ were kindly provided by Stephen R. Ikeda (NIAAA, Rockville, MD), and the Nluc-EPAC-VV plasmid was provided by Kirill Martemyanov (Scripps Research Institute, Jupiter, FL). The Glosensor-22F cAMP plasmid (E2301) was obtained from Promega. Plasmids encoding $G\alpha_s\Delta10$, Venus-Kras, Venus-1–155-$G\gamma_1$, and Venus-155–239-$G\beta_1$ GPCR-luciferase constructs, and p115RhoGEF-Rluc8 have been described previously (6, 15, 36). Plasmids encoding rGFP-CAAX, rGFP-FYVE, and V_2R-RlucII have been described previously (16). PDZ-RhoGEF-RlucII was generated by amplifying the cytosolic G12/13 interacting domain of PDZ-RhoGEF (aa 281–483) with linkerD (GIRLREALKLPAT) on its C terminus which was then subcloned onto the N terminus of RlucII in pcDNA3.1/Zeo(+) by Gibson assembly. GRK2-RlucII D110A was generated by digesting hGRK2-GFP10 D110A and pcDNA3.1/Hygro(+) GFP10-RlucII db v.2 with NheI and HindIII to excise hGRK2 from the former and GFP10 from the latter. hGRK2 was subsequently ligated in frame with pcDNA3.1/Hygro(+) RlucII db v.2 to produce a C-terminal RlucII construct. All plasmid constructs were verified by Sanger sequencing.

Cell Culture and Transfection. HEK 293 cells (ATCC) were propagated in plastic flasks and on 6-well plates according to the supplier's protocol. HEK 293 cells with targeted deletion of *GNAS* and *GNAL* (G$_s$ knockouts; GSKO), targeted deletion of *GNAS*, *GNAL*, *GNAQ*, *GNA11*, *GNA12*, and *GNA13* (G protein three family knockouts; 3GKO), and HEK 293 cells with additional targeted deletions of the 3GKO cells of *GNAI1*, *GNAI2*, *GNAI3*, *GNAT1*, *GNAT2*, *GNAZ*, and *GNAO1* (G protein four family knockouts; 4GKO) were derived, authenticated, and propagated as previously described (9, 10). HEK 293 cells with additional targeted deletion of *ARRB1 and ARRB2* (beta-arrestin knockouts; ARRBKO) were derived, authenticated, and propagated as previously described (37, 38). Cells were transfected in growth medium using linear PEI MAX (MW 40,000) at a nitrogen/phosphate ratio of 20 and were used for experiments 12–48 h later. Up to 3.0 μg of plasmid DNA was transfected in each well of a 6-well plate. For ebBRET experiments, up to 1.0 μg of plasmid DNA was transfected in suspension to a cell density of 350,000 cells/mL in white 96-well plates.

BRET and Luminescence Assays.
Measurement of coupling between receptor and G protein in nucleotide-depleted cells. Cells were transfected with a GPCR-Rluc8 and $G\alpha$ subunit pair, Venus-1–155-$G\gamma_2$, Venus-155–239-$G\beta_1$, and pcDNA3.1(+) or PTX-S1 in a (1:3:1:1:1) ratio. Experiments with $G\alpha_i$ were conducted in 4GKO cells for $G\alpha_i$ cognate receptors and in 3GKO cells for all other receptors. Experiments with $G\alpha_i$ were conducted without PTX-S1; all other $G\alpha$ subunits were cotransfected with PTX-S1. After a 48-h incubation, cells were washed twice with permeabilization buffer (KPS) containing 140 mM KCl, 10 mM NaCl, 1 mM MgCl$_2$, 0.1 mM KEGTA, 20 mM NaHEPES (pH 7.2); permeabilized in KPS buffer containing 10 μg mL^{-1} high-purity digitonin; and transferred to opaque black 96-well plate. Measurements were made from permeabilized cells supplemented either with 100 μM GDP or 2U mL^{-1} apyrase, in both cases with or without agonist (*SI Appendix*, Table S1).
Luciferase complementation. Cells were transfected with a GPCR-SmBit, $G\alpha$, LgBit-$G\gamma_2$, $G\beta_1$, and pcDNA3.1(+) or PTX-S1 in a (1.5:4:1:2.5:3) ratio. After a 24-h incubation, cells were washed twice with DPBS, harvested by trituration, and transferred to opaque white 96-well plates.
GPCR competition assays. Cells were transfected with an untagged GPCR or pcDNA3.1(+), GPCR-Rluc8, $G\alpha$, Venus-1–155-$G\gamma_1$, Venus-155–239-$G\beta_1$, and PTX-S1 in a (10:1:2:2:4) ratio. After a 48-h incubation, cells were washed twice with DPBS, harvested by trituration, and transferred to opaque black 96-well plates.
G protein BRET conformational biosensor. HEK 293 cells were transfected with an untagged GPCR, $G\alpha_{12}$-Rluc8, Venus-1–155-$G\gamma_2$ and Venus-155–239-$G\beta_1$ in a (15:1:4:4) ratio. After a 48-h incubation, cells were washed twice with DPBS, harvested by trituration, and transferred to opaque black 96-well plates.
G_s activation nanoBiT sensor. NanoBiT-G_s protein (39) consisting of $G\alpha_s$ subunit fused with a large fragment (LgBiT) at the alpha-helical domain and an N-terminally small fragment (SmBiT)-fused $G\gamma_2$ subunit along with untagged $G\beta_1$ subunit was expressed in the presence or absence of $G\alpha_{12}$ subunit. HEK 293 cells were seeded in a 6-well culture plate at a concentration of 2×10^5 cells mL^{-1} (2 mL per well in DMEM; Nissui) supplemented with 10% fetal bovine serum (Gibco), glutamine, penicillin, and streptomycin) 1 d before transfection. Transfection solution was prepared by combining 5 μL (per well hereafter) of PEI MAX solution (1 mg mL^{-1}), 200 μL of Opti-MEM (Thermo-Fisher Scientific), and a plasmid mixture consisting of 100 ng LgBiT-containing $G\alpha_s$ subunit, 500 ng $G\beta_1$, 500 ng SmBiT-fused $G\gamma_2$, 100 ng RIC8b, 200 ng untagged V_2R (pCAGGS plasmid) with or without 20 ng $G\alpha_{12}$ subunit (pCAGGS plasmid; gene-synthesized with codon optimization). After

Okashah et al.

incubation for 1 d, transfected cells were harvested with 0.5 mM EDTA-containing DPBS, centrifuged and suspended in 4 mL of HBSS containing 0.01% BSA (fatty acid–free grade; SERVA) and 5 mM Hepes (pH 7.4) (assay buffer). The cell suspension was dispensed in a white 96-well plate at a volume of 80 μL per well and loaded with 20 μL of 50 μM coelenterazine (Carbosynth) diluted in the assay buffer. After 2 h incubation at room temperature, the plate was measured for baseline luminescence (Spectramax L, Molecular Devices), and 20 μL of titrated ligand (AVP) were manually added. The plate was immediately read at room temperature for the following 10 min at a measurement interval of 20 s with an accumulation time of 0.17 s per read. The luminescence counts over 5–10 min after ligand addition were averaged and normalized to the initial count. The fold-change values were further normalized to that of vehicle-treated samples.

Translocation of p115RhoGEF. Cells were transfected with an untagged GPCR, Gα, Gγ$_2$, Gβ$_1$, p115RhoGEF-Rluc8, Venus-Kras, and PTX-S1 in a (2:12:4:4:1:6:2) ratio. After a 48-h incubation, cells were washed twice with DPBS, harvested by trituration, and transferred to opaque black 96-well plates.

Translocation of PDZ-RhoGEF. ΔβARR1/2 HEK 293 cells were transfected with either FLAG-V$_2$R or HA-TPα, Gα$_{12}$, PDZ-RhoGEF-RlucII and rGFP-CAAX in a (8:4:1:12) ratio. After a 48-h incubation, cells were washed once with Tyrode's buffer (140 mM NaCl, 2.7 mM KCl, 1 mM CaCl$_2$, 12 mM NaHCO$_3$, 5.6 mM D-glucose, 0.5 mM MgCl$_2$, 0.37 mM NaH$_2$PO$_4$, 25 mM Hepes [pH 7.4]) and maintained in the same buffer. Cells were stimulated for 5 min with agonist before BRET measurements.

p115-RGS-GFP biosensor to monitor Gα$_{12}$ activity. A BRET-based biosensor composed of RGS homology (RH) domain (amino acids 1–246) of p115Rho-GEF fused to GFP10 (p115-RGS-GFP) and one of two Gα$_{12}$-RlucII fusions (RlucII inserted after amino acid 84 or 136) was used to measure Gα$_{12}$ activity (40). HEK 293 cells were transfected with 40 ng of Gα$_{12}$-RlucII, 500 ng of p115-RGS-GFP, and 300 ng of receptor per row of a 96-well plate. BRET was monitored 2 min after agonist addition.

SRE transcriptional reporter assay. Cells were transfected with a GPCR, Gα subunit, SRE-Luc, and PTX-S1 in a (10:1:100:25) ratio. Medium was exchanged to serum-free 2 h after transfection. After a 24-h incubation, cells were treated with or without agonist for 5 h. Cells were washed twice with DPBS, harvested by trituration, centrifuged at 500 × g for 3 min, and resuspended in equilibration buffer (1× HBSS, 20 mM NaHEPES; pH 7.5) supplemented with 10% FBS by volume, and 2 mM D-luciferin. Cells equilibrated in this solution at room temperature for 30 min and were transferred to opaque white 96-well plates.

NFκB transcriptional reporter assays. Cells were transfected with a GPCR, Gα subunit, NFκB-Luc, and empty vector in a (300:1:300:199) ratio. After a 24-h incubation, cells were treated with or without agonist for 5 h. Cells were washed twice with DPBS, harvested by enzyme-free, centrifuged at 500 × g for 3 min, and resuspended in equilibration buffer (1× HBSS, 20 mM NaHEPES; 0.1% wt/vol BSA, pH 7.5) and transferred into 96-well black/white Isoplates (Perkin-Elmer). Cells were incubated with 2 mM D-luciferin for 30 min before reading luminescence emission at 525 nm after 30 of incubation using a PHERAstar FS (BMG LABTECH).

Nluc-EPAC-VV cAMP assay. Cells were transfected with a pcDNA3.1(+), a GPCR, Gα subunit or pcDNA3.1(+), Gγ$_2$, Gβ$_1$, and Nluc-EPAC-VV in a (59:15:5:15:10:10:1) ratio. After a 24-h incubation, cells were washed twice with DPBS, harvested by trituration, and transferred to opaque black 96-well plates.

Glosensor cAMP assay. GSKO cells were transfected with a GPCR, Gα subunit, Gγ$_2$, Gβ$_1$, Glosensor 22F, and either pcDNA3.1(+) or PTX-S1 in a (1:1:1:1:4:1) ratio. After a 24-h incubation, cells were washed twice with DPBS and treated with trypsin-EDTA (0.05%). Detached cells were harvested and centrifuged at 250 × g for 5 min, and the cell pellet was resuspended in equilibration buffer supplemented with 10% FBS by volume and 2 mM D-luciferin. Cells were incubated at room temperature for 1 h and then distributed to opaque white 96-well plates. Luminescence measurements were made from cells treated with vehicle, agonist, or 100 μM forskolin.

Arrestin recruitment. HEK 293 cells were transfected with a GPCR-Rluc8, Gα, Gγ$_2$, Gβ$_1$, and β-arrestin2–Venus in a (1:2:1:1:1) ratio. After a 24-h incubation, cells were washed twice with DPBS, harvested by trituration, and transferred to opaque black 96-well plates.

Bystander BRET V$_2$R trafficking. HEK 293 cells were transfected with V$_2$R-RlucII, Gα, and either rGFP-CAAX or rGFP-FYVE in a (1:20:60) ratio. After a 48-h incubation, cells were washed once with Tyrode's buffer and maintained in the same buffer. Cells were stimulated for 30 min with agonist before BRET measurements.

HiBiT-based V$_2$R internalization. Parental HEK 293 cells, G$_{12/13}$-deficient HEK 293 cells (39), or β-arrestin1/2-deficient HEK 293 cells (37) in growth phase were seeded in a 6-well culture plate at a concentration of 2 × 10^5 cells mL^{-1}. Cells were transfected with 100 ng of HiBiT-V$_2$R, which contained an Interleukin 6-derived signal sequence followed by a HiBiT sequence and a linker at the N terminus (MNSFSTSAFGPVAFSLGLLLVLPAAFPAPVSGWRLFKKISGGSGGGGSG; gene synthesized with codon optimization) and an unintended SmBiT tag at the C terminus. After 1 d, cells were harvested, suspended in 1 mL of assay buffer, dispensed in a white 96-well half-area plate at a volume of 25 μL per well, and mixed with 25 μL of 2× substrate buffer consisting of 1:200 of a LgBiT stock solution (Promega) and 20 μM furimazine in the assay buffer. After 40 min at room temperature, the plate was measured for baseline luminescence, and a titrated ligand (10 μL) diluted in the 1× substrate buffer was manually added. The plate was immediately read at room temperature for the following 30 min at a measurement interval of 30 s with an accumulation time of 0.4 s per read. The luminescence counts over 27–30 min after ligand addition were averaged and normalized to the initial count.

GRK2 recruitment. For the experiments shown in *SI Appendix*, Fig. S10A, ΔβARR1/2 HEK 293 cells were transfected with FLAG-V$_2$R, GRK2-RlucII D110A, Gα, and GFP-CAAX in a (2:1:2:6) ratio in suspension and distributed into white 96-well plates. After a 48-h incubation, cells were washed once with Tyrode's buffer and maintained in the same buffer. Cells were stimulated with agonist immediately after addition of coelenterazine 400a. For the experiments shown in *SI Appendix*, Fig. S10B, ARRBKO cells were transfected with a GPCR-Rluc8, Gα subunit, Gγ$_2$, Gβ$_1$, and GRK2-Venus in a (1:3:1:1:3) ratio. After a 48-h incubation, cells were washed twice with DPBS, harvested by trituration, and transferred to opaque black 96-well plates.

BRET, luminescence measurements. Steady-state BRET and luminescence measurements were made using a Mithras LB940 photon-counting plate reader (Berthold Technologies GmbH). Kinetic BRET and luminescence time course measurements were made using a Polarstar Optima plate reader (BMG Labtech). Coelenterazine h (5 μM; Nanolight) or furimazine (NanoGlo; 1:1,000, Promega) were added to all wells immediately prior to making measurements with Rluc8 and Nluc, respectively. Raw BRET signals were calculated as the emission intensity at 520–545 nm divided by the emission intensity at 475–495 nm. Net BRET signals were calculated as the raw BRET signal minus the raw BRET signal measured from cells expressing only the Rluc8 donor.

Data Availability. All study data are included in the article and *SI Appendix*.

1. W. I. Weis, B. K. Kobilka, The molecular basis of G protein-coupled receptor activation. *Annu. Rev. Biochem.* **87**, 897–919 (2018).
2. K. L. Pierce, R. T. Premont, R. J. Lefkowitz, Seven-transmembrane receptors. *Nat. Rev. Mol. Cell Biol.* **3**, 639–650 (2002).
3. A. De Lean, J. M. Stadel, R. J. Lefkowitz, A ternary complex model explains the agonist-specific binding properties of the adenylate cyclase-coupled beta-adrenergic receptor. *J. Biol. Chem.* **255**, 7108–7117 (1980).
4. M. E. Maguire, P. M. Van Arsdale, A. G. Gilman, An agonist-specific effect of guanine nucleotides on binding to the beta adrenergic receptor. *Mol. Pharmacol.* **12**, 335–339 (1976).
5. X. J. Yao *et al.*, The effect of ligand efficacy on the formation and stability of a GPCR-G protein complex. *Proc. Natl. Acad. Sci. U.S.A.* **106**, 9501–9506 (2009).
6. N. Okashah *et al.*, Variable G protein determinants of GPCR coupling selectivity. *Proc. Natl. Acad. Sci. U.S.A.* **116**, 12054–12059 (2019).
7. C. Galés *et al.*, Real-time monitoring of receptor and G-protein interactions in living cells. *Nat. Methods* **2**, 177–184 (2005).
8. M. Héroux, M. Hogue, S. Lemieux, M. Bouvier, Functional calcitonin gene-related peptide receptors are formed by the asymmetric assembly of a calcitonin receptor-like receptor homo-oligomer and a monomer of receptor activity-modifying protein-1. *J. Biol. Chem.* **282**, 31610–31620 (2007).
9. Y. Hisano *et al.*, Lysolipid receptor cross-talk regulates lymphatic endothelial junctions in lymph nodes. *J. Exp. Med.* **216**, 1582–1598 (2019).
10. M. Grundmann *et al.*, Lack of beta-arrestin signaling in the absence of active G proteins. *Nat. Commun.* **9**, 341 (2018).

11. J. F. Armstrong *et al.*, The IUPHAR/BPS Guide to PHARMACOLOGY in 2020: Extending immunopharmacology content and introducing the IUPHAR/MMV Guide to MALARIA PHARMACOLOGY. *Nucleic Acids Res.* **48**, D1006–D1021 (2020).

12. S. P. Armstrong, R. M. Seeber, M. A. Ayoub, B. J. Feldman, K. D. G. Pfleger, Characterization of three vasopressin receptor 2 variants: An apparent polymorphism (V266A) and two loss-of-function mutations (R181C and M311V). *PLoS One* **8**, e65885 (2013).

13. M. P. Strathmann, M. I. Simon, G alpha 12 and G alpha 13 subunits define a fourth class of G protein alpha subunits. *Proc. Natl. Acad. Sci. U.S.A.* **88**, 5582–5586 (1991).

14. C. Avet *et al*, Selectivity landscape of 100 therapeutically relevant GPCR profiled by an effector translocation-based BRET platform. *bioRxiv*:2020.04.20.052027 (24 April 2020).

15. T.-H. Lan, Q. Liu, C. Li, G. Wu, N. A. Lambert, Sensitive and high resolution localization and tracking of membrane proteins in live cells with BRET. *Traffic* **13**, 1450–1456 (2012).

16. Y. Namkung *et al.*, Monitoring G protein-coupled receptor and β-arrestin trafficking in live cells using enhanced bystander BRET. *Nat. Commun.* **7**, 12178 (2016).

17. R. Bhattacharyya, P. B. Wedegaertner, Characterization of G alpha 13-dependent plasma membrane recruitment of p115RhoGEF. *Biochem. J.* **371**, 709–720 (2003).

18. M. J. Hart *et al.*, Direct stimulation of the guanine nucleotide exchange activity of p115 RhoGEF by G13. *Science* **280**, 2112–2114 (1998).

19. B. Liu, D. Wu, "Analysis of the coupling of G12/13 to G protein-coupled receptors using a luciferase reporter assay" in *G Protein Signaling*, A. V. Smrcka, Ed. (Humana Press, 2004), pp. 145–150.

20. S. G. F. Rasmussen *et al.*, Crystal structure of the β2 adrenergic receptor-Gs protein complex. *Nature* **477**, 549–555 (2011).

21. J. P. Mahoney, R. K. Sunahara, Mechanistic insights into GPCR-G protein interactions. *Curr. Opin. Struct. Biol.* **41**, 247–254 (2016).

22. R. H. Oakley, S. A. Laporte, J. A. Holt, L. S. Barak, M. G. Caron, Association of β-arrestin with G protein-coupled receptors during clathrin-mediated endocytosis dictates the profile of receptor resensitization. *J. Biol. Chem.* **274**, 32248–32257 (1999).

23. A. R. B. Thomsen *et al.*, GPCR-G protein-β-arrestin super-complex mediates sustained G protein signaling. *Cell* **166**, 907–919 (2016).

24. S. K. Ogden *et al.*, G protein Gαi functions immediately downstream of Smoothened in Hedgehog signalling. *Nature* **456**, 967–970 (2008).

25. K. V. Juul, D. G. Bichet, S. Nielsen, J. P. Nørgaard, The physiological and pathophysiological functions of renal and extrarenal vasopressin V2 receptors. *Am. J. Physiol. Ren. Physiol.* **306**, F931–F940 (2014).

26. E. Klussmann *et al.*, An inhibitory role of Rho in the vasopressin-mediated translocation of aquaporin-2 into cell membranes of renal principal cells. *J. Biol. Chem.* **276**, 20451–20457 (2001).

27. D. P. Staus *et al.*, Regulation of β2-adrenergic receptor function by conformationally selective single-domain intrabodies. *Mol. Pharmacol.* **85**, 472–481 (2014).

28. T. M. Gupte, R. U. Malik, R. F. Sommese, M. Ritt, S. Sivaramakrishnan, Priming GPCR signaling through the synergistic effect of two G proteins. *Proc. Natl. Acad. Sci. U.S.A.* **114**, 3756–3761 (2017).

29. P. Hein, M. Frank, C. Hoffmann, M. J. Lohse, M. Bünemann, Dynamics of receptor/G protein coupling in living cells. *EMBO J.* **24**, 4106–4114 (2005).

30. Y. Du *et al.*, Assembly of a GPCR-G protein complex. *Cell* **177**, 1232–1242.e11 (2019).

31. H. E. Kato *et al.*, Conformational transitions of a neurotensin receptor 1-G$_{i1}$ complex. *Nature* **572**, 80–85 (2019).

32. X. Liu *et al.*, Structural insights into the process of GPCR-G protein Complex Formation. *Cell* **177**, 1243–1251.e12 (2019).

33. G. G. Gregorio *et al.*, Single-molecule analysis of ligand efficacy in β$_2$AR-G-protein activation. *Nature* **547**, 68–73 (2017).

34. W. P. Hausdorff, M. Hnatowich, B. F. O'Dowd, M. G. Caron, R. J. Lefkowitz, A mutation of the β2-adrenergic receptor impairs agonist activation of adenylyl cyclase without affecting high affinity agonist binding. Distinct molecular determinants of the receptor are involved in physical coupling to and functional activation of Gs. *J. Biol. Chem.* **265**, 1388–1393 (1990).

35. T. Kozasa, A. G. Gilman, Purification of recombinant G proteins from Sf9 cells by hexahistidine tagging of associated subunits. Characterization of alpha 12 and inhibition of adenylyl cyclase by alpha z. *J. Biol. Chem.* **270**, 1734–1741 (1995).

36. B. Hollins, S. Kuravi, G. J. Digby, N. A. Lambert, The c-terminus of GRK3 indicates rapid dissociation of G protein heterotrimers. *Cell. Signal.* **21**, 1015–1021 (2009).

37. M. O'Hayre *et al.*, Genetic evidence that β-arrestins are dispensable for the initiation of β2-adrenergic receptor signaling to ERK. *Sci. Signal.* **10**, eaal3395 (2017).

38. L. M. Luttrell *et al.*, Manifold roles of β-arrestins in GPCR signaling elucidated with siRNA and CRISPR/Cas9. *Sci. Signal.* **11**, eaat7650 (2018).

39. A. Inoue *et al.*, Illuminating G-protein-coupling selectivity of GPCRs. *Cell* **177**, 1933–1947.e25 (2019).

40. V. Lukasheva *et al.*, Signal profiling of the β$_1$AR reveals coupling to novel signalling pathways and distinct phenotypic responses mediated by β$_1$AR and β$_2$AR. *Sci. Rep.* **10**, 8779 (2020).